Anal. Chem. **2001,** *73,* 1120−1125

Surface Stoichiometry of Manganin Coatings Prepared by Pulsed Laser Deposition As Described by Laser-Induced Breakdown Spectrometry

L. M. Cabalín and J. J. Laserna*

Department of Analytical Chemistry, Faculty of Sciences, University of Málaga, E-29071 Málaga, Spain

The use of laser-induced breakdown spectrometry (LIBS) for the multielemental distribution of coating samples is discussed. Surface characterization was performed by monitoring plasma emission generated by a Q-switched Nd:YAG laser operating on the second harmonic wavelength at 532 nm. Samples analyzed by LIBS consisted of manganin coatings (Cu, Ni, and Mn) prepared on Si by pulsed laser deposition from a solid manganin target (Cu 86%, Ni 2%, Mn 12%). The thickness of the coating was ∼50 nm. To improve both surface sensitivity and spectral detection, the laser beam was focused 5 mm above the sample surface. A total area of 5.6 mm × 3.5 mm was sampled with a lateral resolution of 375 μm. For quantitative purposes, the data from the coated sample were compared with those obtained from a manganin standard. Significant differences in the stoichiometry of coatings as compared with the original sample were observed.

Surface treatments and coatings are commonly employed by manufacturers throughout the world to increase performance, productivity, and longevity of tools and components.[1,2] The desired coating properties and required performance vary from application to application, thus, increasing the need for a quality control across the surface in all domains of modern science and industry. Information on the physical topography, interfacial morphology, chemical composition, structure, and properties at the surface is obtained from a wide variety of instrumental techniques. As the information provided varies for each method, several complementary techniques have to be employed in relation to the analysis and characterization of surfaces.[3−11]

Laser-induced breakdown spectrometry (LIBS) is gaining acceptance as an alternative method for elemental analysis. LIBS is a simple and fast technique based on laser ablation and ionization of the sample and direct spectral analysis of the microplasma produced. The physical processes involve the laser−material interaction, and its applications have been the subject of numerous publications.[12−20] An interesting capability of LIBS involved rapid, in situ analysis of materials at atmospheric pressure. Derived from this capability, applications for in situ analysis of pollutants and on-line monitoring of specific elements in industrial environments have resulted.[21−23] The development of portable instrumentation[24] is another consequence of this easy-to-use capability. Another feature of LIBS involved the production of analytical information linked to spatial coordinates. At present, strong efforts are being made to develop LIBS in order to improve depth resolution, spatial resolution, detection power, and precision in material analysis.[25−33] St-Onge and Sabsabi obtained quantitative depth profiles using

* To whom correspondence should be sent Fax: 34 952132000. E-mail: (J.J.L.) laserna@uma.es; (L.M.C.) lmcabalin@uma.es.

(1) Anderson D. G. *Anal. Chem*. **1999**, *71*, 21R−32R.
(2) Bengtson, A.; Danielson, L. *Thin Solid Films* **1985**, *231*, 231−238.
(3) Vickerman, J. C. In *Surface Analysis*; Vickerman, J. C., Ed.; John Wiley and Sons: Chichester, U.K., 1997.
(4) Chan, R. W.; Haasen, P.; Kramer, E. J. In *Characterization of Materials*; Lifshin, E., Ed.; VCH Publishers: New York, 1994.
(5) Rivière, J. C.; Myhra, S. In *Handbook of Surface and Interface Analysis*; Rivière, J. C., Myhra, S., Eds.; Marcel Dekker: New York, 1998.
(6) Bengtson, A. *Spectrochim. Acta Part B* **1994**, *49* (4), 411−429.
(7) Jones, D. G. In *Glow Discharge Optical Emission Spectrometry*; Payling, R., Jones, D., Bengtson, A., Eds.; Wiley: Chichester, U.K., 1997; pp 541−546.
(8) Marquardt, B. J.; Stratis, D. N.; Cremer, D. A.; Angel, S. M. *Appl. Spectrosc*. **1998**, *52* (9), 1148−1153.
(9) Bertrand, D.; Devaux, M. F.; Robert, P., *Trends Anal. Chem*. **1991**, *10*, 237−243.
(10) Smith, S. P. In *Secondary Ion Mass Spectrometry*; Wiley: Chichester, U.K., 1997; pp 485−488.
(11) Bhargava, R.; Wall, B. G.; Koenig, J. L. *Appl. Spectrosc. 2000*, *54* (4), 470−479.
(12) Radziemski, L. J. *Microchem. J.* **1994**, *50*, 218−234.
(13) Radziemski, L. J.; Cremers, D. A. In *Laser-Induced Plasmas and Applications*; Radziemski, L. J., Cremers, D. A., Eds,; Marcel Dekker: New York, 1989.
(14) Darker, S. A.; Tyson, J. F. *J. Anal. At. Spectrom*. **1993**, *8*, 145−209.
(15) Schechter, I. *Rev. Anal. Chem*. **1997**, *16* (3), 173−297.
(16) Sneddon, J.; Lee, Y. I. *Anal. Lett*. **1999**, *32* (11), 2143-2162.
(17) Song, K.; Lee, Y. I.; Sneddon, J. *Appl. Spectrosc. Rev*. **1997**, *32* (3), 183−235.
(18) Rusak, D. A.; Castle, B. C.; Smith, B. W.; Winefordner, J. D. *Crit. Rev. Anal. Chem*. **1997**, *27* (4), 257−290.
(19) Winefordner, J. D.; Gornushkin, I. B.; Pappas, D.; Matveev, O. I.; Smith, B. W. *J. Anal. At. Spectrom*. **2000**, *15*, 1161−1189.
(20) Cabalin, L. M.; Laserna, J. J. *Spectrochim. Acta Part B* **1998**, *53*, 723−730.
(21) Ernst, W. E.; Farson, D. F.; Sames, D. J. *Appl. Spectrosc*. **1996**, *50* (3), 306−309.
(22) Bulatov, V.; Gridin, V. V.; Polyak, F.; Schechter, I. *Ana. Chim. Acta* **1997**, *343*, 93−99.
(23) Neuhauser, R. E.; Panne, U.; Niessner, R. *Appl. Spectrosc*. 2000, 54 (6), 923−927.
(24) Yamamoto, K.; Cremer, D. A.; Ferris, M.; Foster, L. *Appl. Spectrosc*. **1996**, *50* (2), 222−233.
(25) St-Onge, L.; Sabsabi, M. *Spectrochim. Acta B* **2000**, *55*, 299−308.
(26) Vadillo, J. M.; Garcia, C. C.; Palanco, S.; Laserna J. J. *J. Anal. At. Spectrom*. **1998**, *13*, 793−797.
(27) Vadillo, J. M.; Palanco, S.; Romero, D.; Laserna, J. J. *Fresenius. J. Anal. Chem*. **1996**, *355*, 909−912.
(28) Vadillo, J. M.; Laserna, J. J. *J. Anal. At. Spectrom*. **1997**, *12*, 859−862.
(29) Anglos, D.; Couris, S.; Fotakis, C. *Appl. Spectrosc*. **1997**, *51*, 1025−1030.
(30) Palanco, S.; Cabalin, L. M.; Romero, D.; Laserna, J. J. *J. Anal. At. Spectrom*. **1999**, *14*, 1883−1887.
(31) Anderson, D. R.; McLeod, C. W.; English, T.; Smith, A. T. *Appl. Spectrosc*. **1995**, *49*, 691−701.
(32) St-Onge, L.; Sabsabi, M.; Cielo, P. *J. Anal. At. Spectrom*. **1997**, *12*, 997−1004.
(33) Lorenzen, C. J.; Carlhoff, C.; Hahn, U.; Jogwich, M. *J. Anal. At. Spectrom*. **1992**, *7*, 1029−1035.

10.1021/ac000715k CCC: $20.00
Published on Web 02/20/2001

LIBS of galvannealed coating on steel by testing different calibration strategies.[25] The Gaussian energy distribution of laser beams normally used in LIBS limits the depth resolution of the technique. Some interesting developments in this area have been reported. A 308-nm collimated beam has been utilized to obtain flat ablated profiles in Zn-coated steel.[26] This approach resulted in an improvement in the depth resolution compared to the focused configuration. The sampling depth was 8 nm pulse^{-1}. The feasibility of LIBS for depth profiling from samples with different phosphorus diffusion steps in silicon wafers has been demonstrated.[34] In this case, the laser was focused at the surface and the sampling depth was 1.2 μm pulse^{-1}. The effect of laser fluence on the LIBS sensitivity was studied by Hidalgo et al.[35] It was shown that surface sensitivity increases with decreasing laser fluence. Advancement in the investigations has resulted in the development of LIBS to produce analytical data in image form. Three-dimensional compositional information can be obtained by combining lateral profiles of the analyzed area with depth-profiling capabilities. 3D distribution of various pigments of paper coatings have been reported.[36,37] The imaging capability of LIBS has been also demonstrated for testing the impurities distribution on photonic-grade silicon samples,[38,39] for the analysis of elemental distribution in polished rock samples,[40] and for the determination of copper in a printed circuit board.[41] Recently, volume distribution of platinum group metals in automotive catalytic converters has been demonstrated.[42] A new approach for compositional mapping of solar cells was tested.[43] The basic idea relies on focusing the laser beam with a cylindrical lens to produce long and narrow microline plasma. With this approach, the speed of analysis was improved by 25-fold compared to conventional LIBS configuration. While most LIBS data describe the distribution of elements in qualitative form, no quantitative information in image format has been reported so far.

In this work, LIBS is presented for the quantitative surface characterization of manganin coatings applied on a Si substrate by pulsed laser deposition. The effects of pulse energy and beam focal conditions of the analysis laser on surface sensitivity, depth resolution, and lateral resolution have been examined. Compositional distribution maps of Mn, Cu, and Ni on the analyzed surface are shown. Images on binary format created by LIBS of the manganin distribution across the coating are also presented. The results indicate that the surface stoichiometry of the coating differs in wide surface areas from the original composition of the manganin standard. These results are in good agreement with those obtained by energy-dispersive X-ray microprobe analysis.

EXPERIMENTAL SECTION

A schematic diagram of the LIBS experimental setup employed in this study has been reported previously in detail.[44] Therefore, only a brief description will be given here. The second harmonic of a pulsed Nd:YAG laser (Continuum, model Surelite SLI-20, λ = 532 nm, pulse width 5 ns) was used to generate sample plasmas. The pulse energy output was measured with a pyroelectric joulemeter (Gentec, model ED-200, with a nominal sensitivity of 9.86 V J^{-1}) coupled with a digital oscilloscope. The laser energies studied were from 1.5 to 25 mJ pulse^{-1} with a pulse repetition rate of 1 Hz. The experiments were carried out in air at atmospheric pressure. The beam was guided with a quartz prism and focused, at normal incidence, on the sample surface with a biconvex quartz lens with a focal length of 100 mm and f number of 4. The focusing lens was mounted on a vertical translation stage so that the lens−target distance could be changed. Beam diameter was measured by displacing a slit through the focal position and measuring the transmitted light with a joulemeter. With this method, in the focal point the laser spot diameter was estimated to be ∼125 μm. Plasma light collection was performed with a quartz planoconvex lens with focal length of 100 mm and f number of 4 into the entrance slit of a 0.5-m focal length Czerny-Turner spectrograph (Chromex, model 500 IS, with three indexable gratings of 300, 1200, and 2400 grooves mm^{-1}). Light was dispersed using the 2400 grooves mm^{-1} grating. The reciprocal linear dispersion was 2.5 nm mm^{-1}. The entrance slit was 10 μm wide and the height was 10 mm. The dispersed light was detected using a two-dimensional charge-coupled device (CCD) detector (Stanford Computer Optics, model 4Quik 05) equipped with an intensifier system. The CCD consists of 768 (h) × 512 (v) elements. The photoactive area is 6 × 4.5 mm^2. The spectral resolution of system was 0.02 nm pixel^{-1}. With this configuration, each spectrum covers ∼15 nm. The spectral region covering the range of 292−307 nm was chosen. Operation of the detector was controlled by 4 Spec 1.20 software. The emission signal was corrected by subtraction of the dark signal of the detector, which was separately measured for the same exposure time. Each pulse was stored as a file containing spectral and spatial information. Calibration of the detector system was conducted by using the lines emitted from titanium laser-induced plasma.

For the sake of comparison, a scanning electronic microscope (SEM) (JEOL, model JSM-6400) equipped with a microprobe (Link Analytical, model EXL), which allowed the compositional analysis, with an acceleration voltage of 20 kV, was also employed.

Samples. Samples consisted of a thin coating of manganin (Cu, Ni, and Mn) on a Si substrate. The samples were prepared by laser-induced evaporation of a solid manganin target (Cu 86%, Ni 2%, Mn 12%) and were supplied by the Bremer Institut für Angewandte Strahltechnik (Bremen, Germany). With this method, the coating thickness was of ∼50 nm. This value was measured using energy-dispersive X-ray (EDX) spectrometry. The samples were placed on a manual $X-Y-Z$ translation stage to be moved with respect to the laser.

RESULTS AND DISCUSSION

Spectral Analysis and Surface Sensitivity. Compositional mapping by LIBS describes the distribution of one or several

(34) Milán, M.; Lucena, P.; Cabalín, L. M.; Laserna, J. J. *Appl. Spectrosc.* **1998**, *52*, 444−448.
(35) Hidalgo, M.; Martin, F.; Laserna, J. J. *Anal. Chem.* **1996**, *68*, 1095−1100.
(36) Häkkänen, H. J.; Korppi-Tommola, J. E. I. *Appl. Spectrosc.* **1995**, *49*, 1721−1728.
(37) Häkkänen, H. J.; Korppi-Tommola, J. E. I. *Anal. Chem.* **1998**, *70*, 4724−4729.
(38) Romero, D.; Laserna, J. J. *Anal. Chem.* **1997**, *69*, 2871−2876.
(39) Romero, D.; Laserna, J. J. *J. Anal. At. Spectrom.* **1998**, *13*, 557−560.
(40) Yoon, Y. Y.; Kim, T. S.; Chung, K. S.; Lee, K. Y.; Lee, G. H. *Analyst* **1997**, *122*, 1223−1227.
(41) Kim, T.; Lin, C. T.; Yoon, Y. *J. Phys. Chem. B* **1998**, *102*, 4284−4287.
(42) Lucena P.; Vadillo J. M.; Laserna J. J. *Anal. Chem.* **1999**, *71*, *1*, 4385−4391.
(43) Mateo, M. P.; Palanco, S.; Vadillo; J. M.; Laserna, J. J. *Appl. Spectrosc.* **2000**, *54* (10), 1429−1434.
(44) Romero, D.; Fernández Romero, J. M.; Laserna, J. J. *J. Anal. At. Spectrom.* **1999**, *14*, 199−204.

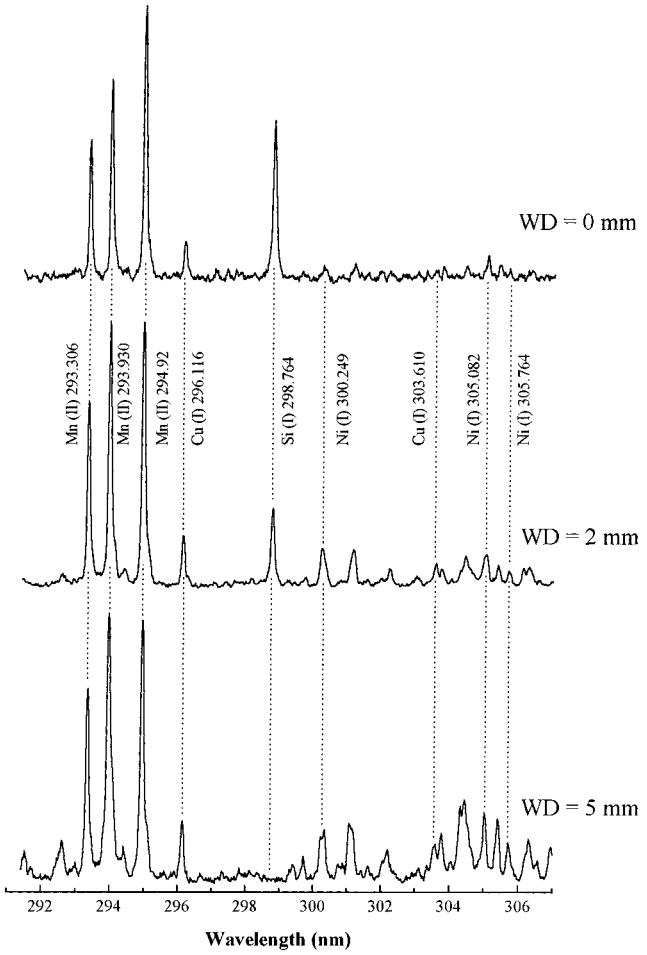

Figure 1. Comparison of single-shot LIB spectra of manganin on Si substrate at three different working distances for $\lambda = 532$ nm. The laser energy was 7 mJ pulse^{-1}. The acquisition time and delay time were of 1 μs and 750 ns, respectively.

constituents on a solid surface by monitoring emission lines from the sample plasma. For multicomponent samples, an adequate spectral range must be selected, while the variables affecting the signal acquisition have to be optimized. For the present sample, a spectral window covering the range 292−307 nm was chosen since all manganin elements and the Si substrate could be measured simultaneously. The intense and well-resolved emission lines of Mn (II) at 294.920 nm, Cu (I) at 296.116 nm, Ni (I) at 300.249 nm, and Si (I) at 298.764 nm were selected.

An important aspect of LIBS imaging is the relationship between spatial resolution and spectral detection. The depth resolution plays a crucial role in the characterization of coatings with thickness in the order of nanometers. The ablation depth reached by a single nanosecond laser pulse can vary from a few micrometers to some nanometers depending on the beam focal conditions, the laser pulse energy, and the properties of ablated material.[31,44,45] For this reason, a preliminary study of both variables (working distance, WD, and laser energy) was carried out in order to reach the best depth resolution with an acceptable level of lateral resolution and good surface sensitivity. The effect of WD on surface sensitivity is well illustrated in Figure 1. Single-shot LIB spectra of the manganin-coated sample corresponding to three different working distances are shown. Variable focal conditions were achieved by shifting the focusing lens relative to the sample surface. In the figure, a WD of zero denotes that laser beam was focused at the sample surface while positive values of WD refer to the beam laser being focused at a position above the coating surface. As shown, at WD = 0 and WD = 2, emission lines from the manganin components and from the silicon substrate appear. This fact indicates that both structural components are being ablated and contribute to the observed spectrum. However, there is no evidence of Si when working at WD = 5, confirming both good surface sensitivity and satisfactory spectral detection under these conditions. Further increase in WD results in an improved depth resolution at the expense of spectral sensitivity while sacrificing even more the lateral resolution. The ratios of the manganin constituent signals to the silicon signal as a function of beam focal conditions for a laser energy of 9 mJ pulse^{-1} are shown in Figure 2a. Only positive values of WD were tested, since previous work indicated that when the laser beam is focused below the sample surface the ablation process occurs

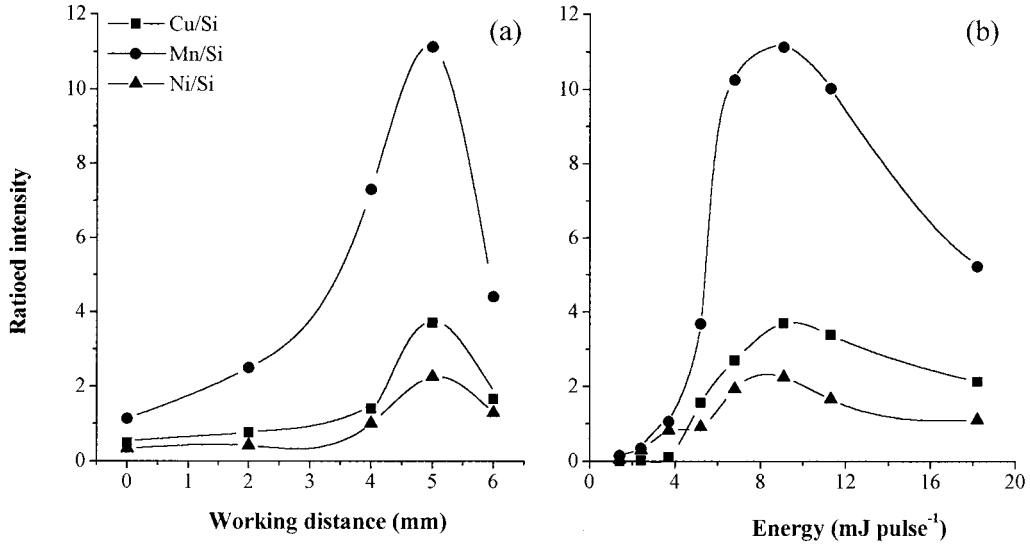

Figure 2. Variation of relative LIB intensity as a function of (a) working distance at 9 mJ pulse^{-1} and (b) incident laser energy at WD = 5 mm for (■) Cu at 296.116 nm, (●) Mn(II) at 294.92 nm, and (▲) Ni (I) at 300.249 nm, ratio to Si (I) at 298.764 nm. The emission signal was measured from each single laser shot.

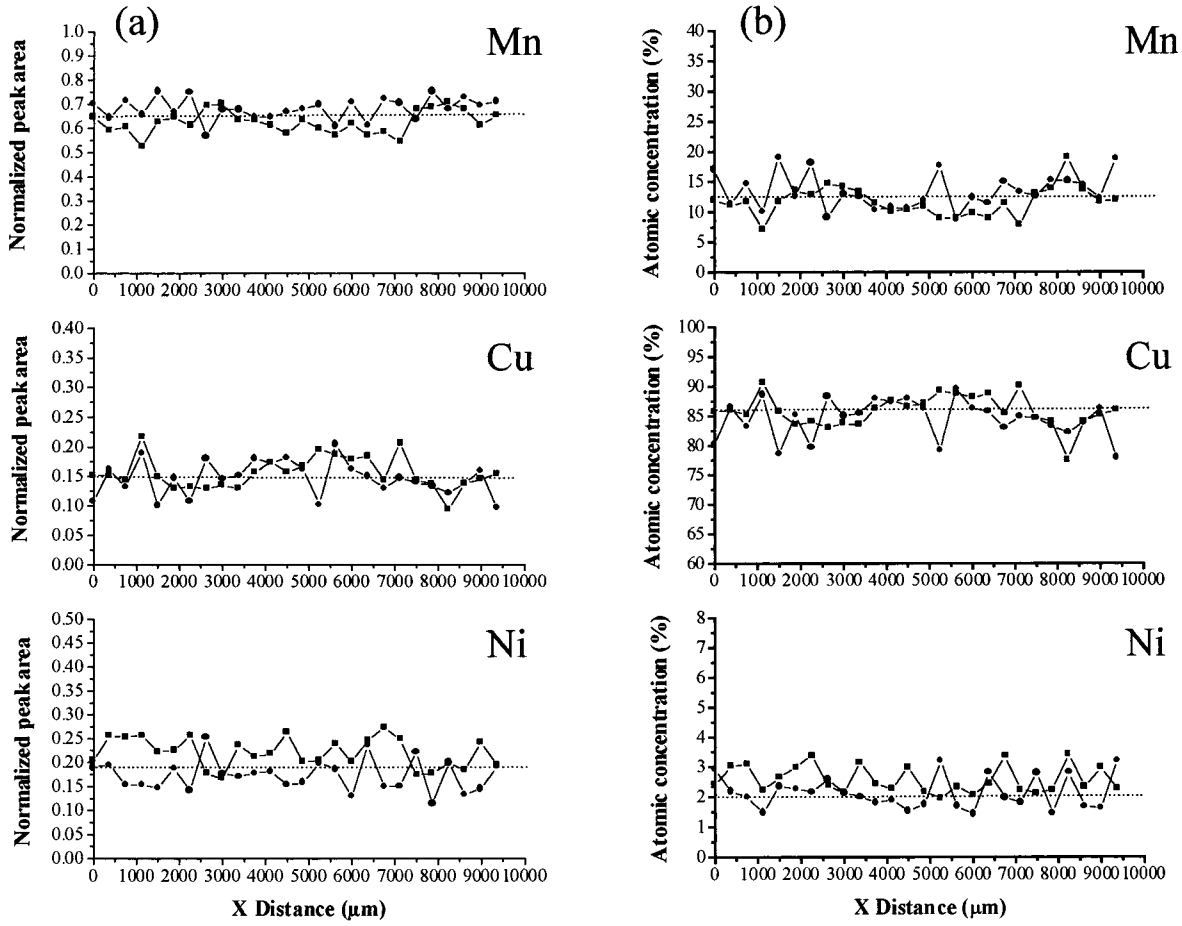

Figure 3. Lateral profiles separated by 3 mm for Mn, Cu, and Ni expressed as (a) normalized peak areas and (b) atomic concentration (%). The dashed lines correspond to the respective averaged values from a manganin standard. Data were acquired by accumulating four laser shots on each sampling position. The laser energy was 7 mJ pulse^{-1}. WD = 5 mm. Other conditions as in Figure 1.

at both sides of the focal position, and under those circumstances, a larger amount of material is ablated thus deteriorating the depth resolution.[38] No air breakdown was observed at the energy levels used in this experiment. As shown in Figure 2a, the relative signals increase with WD for the three elements and reach a maximum by focusing the beam 5 mm above the sample surface. This effect derives from the larger area sampled and explains the improved ratio of signal intensities observed.

The effect of laser energy on the relative signals for Mn, Cu, and Ni is also shown for a WD of +5 mm in Figure 2b. As shown, a larger laser energy improved the spectral detection up to a value of 9 mJ pulse^{-1}. At higher energies, the signal tends to decrease due both to plasma shielding from the ablated material in front of the sample surface and to air breakdown, which occurs at ~9.2 mJ pulse^{-1} in this experiment. On the other hand, lateral and depth resolutions deteriorated with energy. As a compromise between depth resolution and spectral sensitivity, a laser energy of 7 mJ pulse^{-1} and a WD of +5 mm were chosen as the most adequate operating conditions and employed for compositional mapping of manganin on the Si substrate.

Surface Distribution of Manganin Constituents on Si. To check the surface distribution of the individual manganin constituents on silicon, two rasters of 26 consecutive positions along the manganin coating on the Si substrate were analyzed. Since internal standardization cannot be used in this kind of sample, peak areas from each element were normalized to sum peak areas of Mn, Cu, and Ni. To ensure the total removal of manganin coating, four laser shots were accumulated at each sampling position. Figure 3a shows the lateral profiles for Mn, Cu, and Ni. Data were acquired at 375-μm intervals along the X axis with the rasters separated by 3 mm. To distinguish the fluctuations in intensity caused by laser−material interaction from those due to compositional differences along the profiles, the normalized peak areas obtained from a manganin target standard were also measured. The averaged signal for each manganin constituent is presented in Figure 3a as a dashed line. Relative standard deviation (RSD) values corresponding to normalized peak areas of manganin components were calculated for both the standard solid sample and the coated sample. In the standard sample, the RSD for Mn was 2%, while for Cu and Ni the values were quite higher, 11 and 7%, respectively, due to the lower sensitivity of the spectral lines used. The Mn, Cu, and Ni normalized peak areas in the coated sample exhibit RSD values of 7, 20, and 17%, which are significantly higher than the precision observed for the standard sample. While this fact was expected since the standard is a bulk sample, the poorer precision with the coated sample can be interpreted as due to the existence of a variation in coating composition with distance.

These results are confirmed by the lateral profiles of the three elements expressed as atomic concentration. The results are shown in Figure 3b. The conversion from normalized peak area to atomic concentration was performed by comparing the values obtained from the manganin-coated sample with those obtained

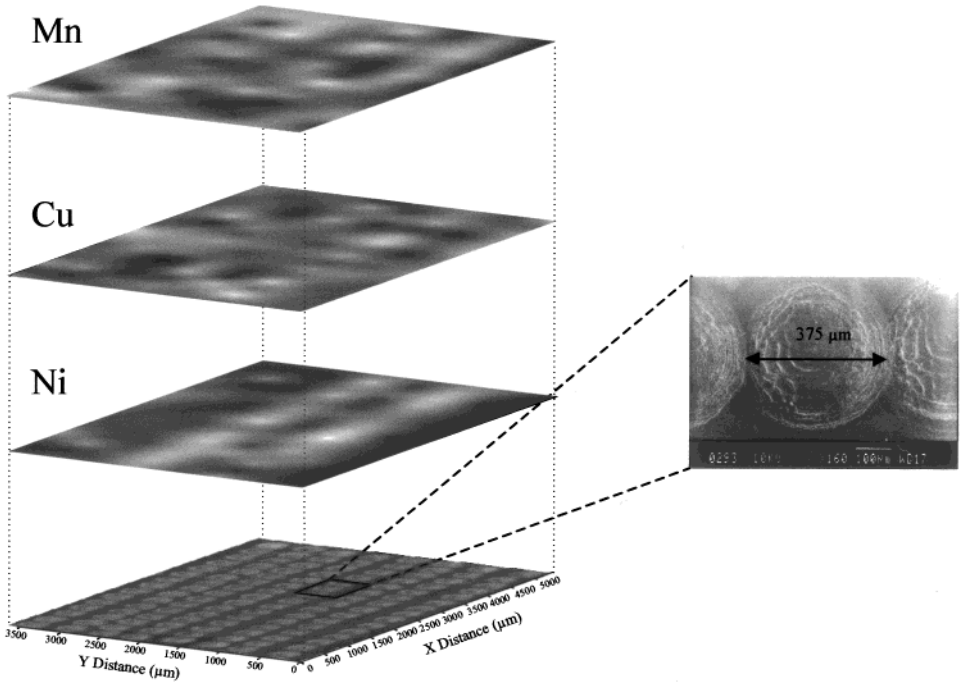

Figure 4. LIBS images of the spatial distribution of Mn, Cu, and Ni. A digitized image of the sample surface analyzed by LIBS is also shown. Data were acquired by accumulating four laser shots on each sampling position. The inset shows a SEM micrograph of the crater formed after 10 laser shots. Other conditions as in Figure 3.

from a manganin standard and then calculating the atomic concentrations considering that the sum of Mn, Cu, and Ni concentration is 100%. This approach assumed that the ablation efficiency and emitted light are similar for the standard and the sample matrix. Consequently, differences in atomic concentration across the coating could indicate the spatial stoichiometric change in the manganin elements deposited by PLD on the Si substrate. The results in Figure 3b indicate that depending to the position the composition of the coating deviates from that in the manganin standard. The deviation is very large in some instances and affects the three elements.

The lateral profiles of Figure 3, although capable of providing an accurate description of compositional changes, are not appropriate when a large area has to be analyzed. Chemical maps of Mn, Cu, and Ni on the Si substrate were then acquired for a wide surface area. A total area of 5.6×3.5 mm^2 was sampled in a sequence of 15 positions separated by 375 μm in the horizontal direction, while 7 parallel rasters separated by 500 μm were executed in the vertical direction. The results are shown in Figure 4. For comparative purposes, a digitized image of the area examined is also presented. The inset shows a detail of the craters produced. The LIBS images represent the normalized peak areas to sum of peak areas. The gray-level scale was adjusted by using a data-processing algorithm which divided the acquired signal into four or more levels and assigned black as the level of lowest relative peak area and white as the highest, with gray levels in between. In Figure 4, dark zones indicate a deficiency of one element while at the same sampling site the concentration of the other constituents seems to be increased. These results demonstrate a significant heterogeneity in the distribution of manganin elements on the Si substrate.

Recognition of Constituent Relationships. While the gray scale maps of Figure 4 are useful for displaying the compositional differences across the surface of the individual manganin constituents, there is no ready way to superimpose the data to indicate the zones where the manganin composition is maintained in the coating. For disclosing the relationship between elements, a two-step procedure was used which involved first selecting the sampling points lying within a specified concentration range and then tracing back these points to the original locations on the sample surface. For the first task, a ternary concentration histogram (CH)[46] was prepared from the three compositional maps in Figure 4. Data were then replotted as shown in Figure 5, where each point represents a position in the original image with a par-

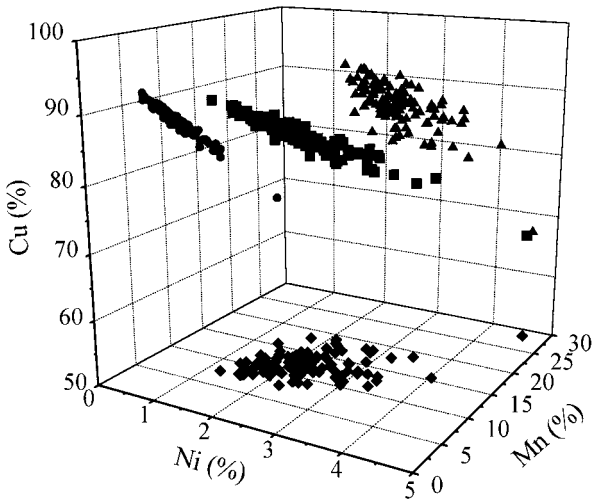

Figure 5. Ternary concentration histogram corresponding to Mn, Cu, and Ni of the manganin-coated sample (Figure 4): (■) with atomic concentration of Ni (%) on the *x*-axis, atomic concentration of Mn (%) on the *y*-axis, and atomic concentration of Cu (%) on the *z*-axis; (◆) *X*−*Y* projection; (▲) *X*−*Z* projection; and (●) *Y*−*Z* projection. The conversion of normalized peak area to atomic concentration is described in the text.

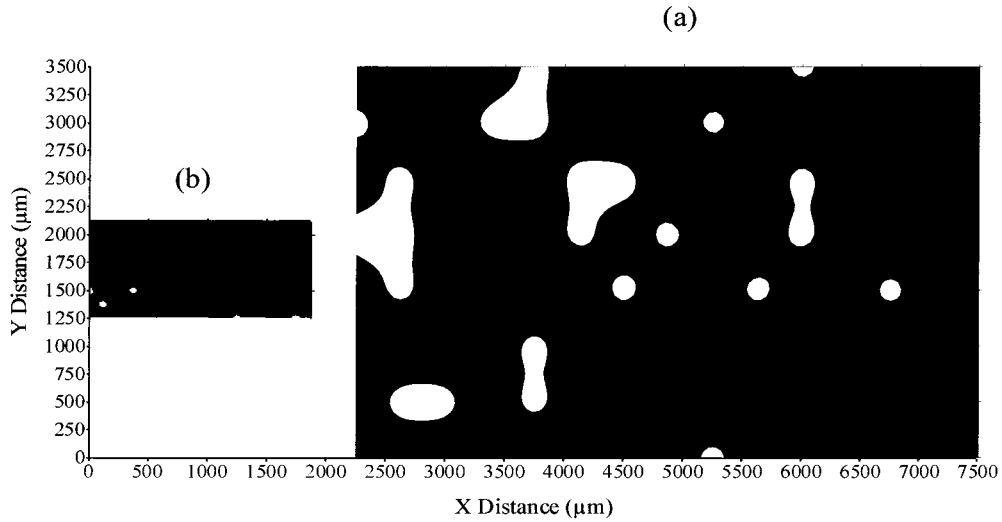

Figure 6. Binary images generated (a) from the LIBS data of Figure 5 indicating the surface distribution of manganin on the sample and (b) from EDXS concentration data.

ticular set of concentration values. The binary histogram presented as projections of manganin atomic concentration on the sides of the plot help discern the three-dimensional shape of the ternary CH. As shown, the data are clustered around the nominal concentration of manganin (86% Cu, 12% Mn, 2% Ni), but the compositional variability of the points is significant. For the second task, the point values were selected on the basis of a homogeneous criterion for which the composition for the three elements simultaneously deviated no more than 10% atomic concentration from the manganin standard (i.e., 86 ± 8.6% for Cu; 12 ± 1.2% for Mn; 2 ± 0.2% for Ni). This approach should be considered only as semiquantitative since a large deviation from the nominal concentration is allowed. However, for comparative purposes, the approach will suffice. Later, the data were processed to assign logical values of true or false at each position analyzed. This data-processing algorithm results in the binary image shown in Figure 6a, where white indicates the locations with concentration values lying in the specified concentration range (true), while black is assigned to positions lying outside the concentration range (false). In Figure 6a, the locations in the coating where the atomic concentrations are close to manganin values can be now readily identified. Indeed, few locations can be said to correspond to the original manganin stoichiometry.

To confirm the spatial stoichiometric change disclosed by LIBS, and as the area analyzed was damaged, an adjacent zone was examined by energy-dispersive X-ray microprobe analysis (EDXS). As in LIBS, a sequence of 16 positions in the longitudinal direction and 8 repetitive sequences in the vertical direction were examined. Due to the characteristics of EDXS method, the operating conditions differed in terms of lateral resolution (50−100 nm) and separation between measurements (125 μm) with respect to those used in LIBS. Consequently, the resulting scanned area was only 1.875 × 0.875 mm^2. The EDXS concentration data were processed according to the mathematical algorithm described above for LIBS. The resulting binary image of the manganin coating is shown in Figure 6b. It should be noted that parts a and b of Figure 6 are to scale. As shown, only limited regions in the coating exhibit the stoichiometry of the original manganin. This result agrees with the results given by LIBS. When compared to the LIBS map, the EDXS data are confined to smaller areas but still reveal the heterogeneous nature of the coating within the allowed concentration variability.

CONCLUSIONS

The present work demonstrates the capabilities of LIBS for generating rapid and simultaneous multielemental maps of sample constituents without sample preparation. The sensitivity, selectivity, and versatility of this analytical approach makes it ideal for surface characterization and depth profiling of manufactured samples. The results indicate that the laser focal conditions and laser pulse energy are important parameters determining lateral resolution, depth resolution, and surface sensitivity. With the choice of the appropriate operating conditions, the technique has been successfully applied to surface characterization in a semiquantitative basis. Composition maps generated by LIBS provide visual information of the spatial distribution of individual coating constituents. However, the recognition of constituent relationships requires extensive postprocessing of the data as with other surface-imaging techniques.

ACKNOWLEDGMENT

This work was supported by Project PB97-1107 of the Dirección General de Investigación Científica y Técnica (Ministry of Education and Culture, Madrid, Spain). The authors are grateful to the Bremer Institut für Angewandte Strahltechnik (BIAS) for the preparation and supplying of the manganin samples and to Prof. J. Pascual for the energy-dispersive X-ray microprobe data. L.M.C. is also grateful to the Spanish Secretaría de Estado de Universidades, Investigación y Desarrollo for providing a postdoctoral fellowship.

(45) Cabalin, L. M.; Romero, D.; Baena, J. M.; Laserna, J. J. *Fresenius J. Anal. Chem.* **1999**, *365*, 404−408.

(46) Williams, D. B.; Pelton, A. R.; Gronsky, R. In *Images of Materials*; Williams, D. B., Pelton, A. R., Gronsky, R., Eds.; Oxford University Press: New York, 1991; p 298.

Received for review June 21, 2000. Accepted December 19, 2000.

AC000715K